Improving Transient Performance in Computationally Simple Gyro-Corrected Satellite Attitude Determination

Anton de Ruiter,[†]
Carleton University, Ottawa, ON, Canada

This paper extends a previously presented Kalman-like filter for fusing gyro measurements with attitude measurements obtained from external sensors such as star-trackers, magnetometers and sun-sensors. The simplicity of this approach is useful for applications such as micro-/nano-satellites where computational power is limited. The previously presented filter uses constant filter gains. It was shown that by appropriately choosing the constant gains, near-optimal steady-state performance is obtained. A drawback of using constant gains is that optimal transient filter performance is lost, meaning that convergence is slower. In this paper, a computationally simple analytical approximation to the transient part of the Kalman filter gain is derived, allowing the transient performance to be recovered. The transient approximation of the gain is then applied for a predetermined fixed period of time, after which the gain is switched to the previously presented constant steady-state Kalman gain. A simple expression for a suitable time to switch from transient to steady-state filter operation is derived. Simulation results demonstrate the efficacy of this approach.

Keywords: spacecraft attitude determination, computational simplicity, Kalman filtering

I. Introduction

Almost all satellite missions require the capability to determine the satellite attitude, often very accurately. It is well-known that gyros provide very low-noise measurements at a high data rate, but suffer from drift resulting in unbounded attitude errors [1]. On the other hand, measurements obtained from ``external'' sensors such as magnetometers, sun-sensors and star-trackers provide more noisy measurements at a much lower data rate with bounded errors. Low noise attitude estimates with bounded errors can be obtained at a high rate by appropriate fusion of the gyro and external attitude measurements.

The Kalman filter, which provides minimum error variance estimates, is fundamental to several sophisticated data fusion techniques [2,3]. A good survey of several different methods applied to spacecraft attitude determination can be found in reference [3]. A limitation of a number of these methods is their computational complexity, making them less suitable for satellites with limited computational capability, such as micro-/nano-satellite applications (for example the JC2Sat nanosatellite formation flying mission [4]). Another approach that has recently been developed for gyro-correction in the attitude determination problem is a nonlinear observer [5-7]. The nonlinear observers presented in [5-7] are computationally much simpler, since only constant gains are required. In [8], the observer obtained in [5] is generalized, and it is shown that the steady-state Kalman filter (with constant gains) may be implemented in this framework in closed-loop form [1]. As shown in [8], the resulting filter is computationally simple to implement, and provides near-optimal

[†] Assistant Professor, Department of Mechanical and Aerospace Engineering

steady-state performance. The steady-state performance is guaranteed provided the spacecraft body-rate is constant.

The cost of using a constant gain to achieve optimal steady-state performance is deteriorated initial transient performance (slower convergence). In many cases, the initial attitude error and gyro bias estimate error are small enough that a linearization of the dynamics is valid. The work in this paper is complementary to the work presented in [8]. The contribution of this paper is a computationally simple analytical approximation to the transient part of the optimal Kalman filter gain matrix, which recovers the transient performance of the optimal Kalman filter for the spacecraft attitude determination problem. By initially implementing the transient approximation developed in this paper followed by the constant gain from [8] after a predetermined switching time, filter performance that is very similar to the optimal Kalman Filter can be obtained both in transient and steady-state. That is, the resulting filter has rapid convergence, and small steady-state error.

As in [8], it is assumed that a full three-axis attitude measurement is available. There are several methods by which this can be performed [9-11], and the details are not considered in this paper.

This paper is organized as follows: section II presents the transient approximation to the Kalman gain, section III demonstrates the results with a numerical example and section IV presents the conclusions.

II. Transient Behavior of Attitude Error Equations

It has been shown in [8] that when implemented as a nonlinear observer [5], the steady-state Kalman filter for the spacecraft attitude determination problem has a very simple form and is globally stabilizing with exponential convergence. The benefits of this are two-fold. First, it is computationally inexpensive to implement, since only two scalar constant gains to be stored (k_p and k_b). Second, the stability is global, which cannot be guaranteed for more general Extended Kalman filter implementations when applied to a nonlinear system such as the gyro error equations [3].

The penalty of implementing such a constant filter is that the transient behavior of the optimal Kalman filter (provided the initial state estimate is small enough that the linearization holds) is lost. This results in longer settling times, as is shown in the example in section IV. In general, if an external measurement of the attitude is available, as is necessary for the filter in this paper, it may be used to initialize the filter, and as such, the initial attitude error will not be large. Therefore, the linearized error equations can be considered in order to find a suitable transient approximation to the optimal Kalman gain, and speed up the resulting filter convergence.

It was shown in [16] that for integrated GPS/INS problems for position and velocity determination, this transient performance may be recovered by a suboptimal filter implementation as follows. Consider the linear time-invariant system

$$\dot{\boldsymbol{x}} = \mathrm{A}\boldsymbol{x} + \boldsymbol{w}, \tag{1}$$

with measurements

$$\boldsymbol{y} = \mathbf{H}\boldsymbol{x} + \boldsymbol{v}\,, \tag{2}$$

where $E\{\boldsymbol{w}(t)\} = \boldsymbol{0}$, $E\{\boldsymbol{v}(t)\} = \boldsymbol{0}$, $E\{\boldsymbol{w}(t)\boldsymbol{w}^T(\tau)\} = \mathbf{Q}\delta(t-\tau)$ and $E\{\boldsymbol{v}(t)\boldsymbol{v}^T(\tau)\} = \mathbf{R}\delta(t-\tau)$. The transient filter behavior of the optimal Kalman filter may be recovered by using the filter gain

$$\mathbf{K} = \begin{cases} \hat{\mathbf{K}}(t), & 0 \le t \le t^* \\ \mathbf{K}_{ss}, & t > t^* \end{cases} \tag{3}$$

where t^* is a predetermined time denoting a switch from transient to steady-state operation, $\mathbf{K}_{ss}$ is a constant gain and $\hat{\mathbf{K}}(t) \approx \mathbf{K}_{kal}(t)$ is an approximation to the transient part of the optimal Kalman gain. Note that the optimal Kalman gain satisfies

$$\begin{aligned} &\mathbf{K}_{kal}(t) = \mathbf{P}(t)\mathbf{H}^T\mathbf{R}^{-1} \\ &\dot{\mathbf{P}} = \mathbf{AP} + \mathbf{PA}^T - \mathbf{PH}^T\mathbf{R}^{-1}\mathbf{HP} + \mathbf{Q}, \quad \mathbf{P}(0) = \mathbf{P}_0, \end{aligned} \tag{4}$$

where $\mathbf{P} = E\{\boldsymbol{x}\boldsymbol{x}^T\}$.

In this section, an approximation of the form of (10) for the Kalman gain is obtained for the attitude determination problem to improve the transient filter performance (faster settling time). A suitable time to switch from transient to steady-state filter operation is also derived. The steady-state part of the filter is covered by reference [8].

First, similar to [16], an approximation on the initial error covariance is made. That is, for $\mathbf{P}_0 >> \mathbf{P}_{ss}$, the error variance is driven by the initial uncertainty, rather than the process noise $\mathbf{Q}$, so that for $0 \le t \le t^*$, for some to be determined t^*, the covariance approximately satisfies (compare to (11))

$$\dot{\mathbf{P}} = \mathbf{AP} + \mathbf{PA}^T - \mathbf{PH}^T\mathbf{R}^{-1}\mathbf{HP}, \quad \mathbf{P}(0) = \mathbf{P}_0\,. \tag{5}$$

After the time t^*, the filter is considered to be in steady-state operation, and $\mathbf{P} \approx \mathbf{P}_{ss}$, where

$$\mathbf{AP}_{ss} + \mathbf{P}_{ss}\mathbf{A}^T - \mathbf{P}_{ss}\mathbf{H}^T\mathbf{R}^{-1}\mathbf{HP}_{ss} + \mathbf{Q} = \mathbf{0} \tag{6}$$

If the state-transition matrix $\mathbf{\Phi}(t)$ can be found for the general first order linear system

$$\dot{\boldsymbol{x}} = \mathbf{A}\boldsymbol{x} \tag{7}$$

satisfying

$$\dot{\mathbf{\Phi}} = \mathbf{A\Phi}, \quad \mathbf{\Phi}(0) = \mathbf{I}\,, \tag{8}$$

it can be readily shown that provided $\mathbf{P}_0 > \mathbf{0}$, the solution to (12) is given by

$$\mathbf{P}(t) = \mathbf{\Phi}(t)\left(\mathbf{P}_0^{-1} + \int_0^t \mathbf{\Phi}^T(\tau)\mathbf{H}^T\mathbf{R}^{-1}\mathbf{H}\mathbf{\Phi}(\tau)d\tau\right)^{-1}\mathbf{\Phi}^T(t)\,. \tag{9}$$

The approximate filter gain is then given by

$$\hat{\mathbf{K}}(t) = \mathbf{P}(t)\mathbf{H}^T\mathbf{R}^{-1}$$
$$\mathbf{P}(t) = \mathbf{\Phi}(t)\left(\mathbf{P}_0^{-1} + \int_0^t \mathbf{\Phi}^T(\tau)\mathbf{H}^T\mathbf{R}^{-1}\mathbf{H}\mathbf{\Phi}(\tau)d\tau\right)^{-1}\mathbf{\Phi}^T(t) \tag{10}$$

From (17) and (15), it is clear the filter gain depends upon the open loop system, and as such it may be computed offline. As shown in [8], for the filter design with small attitude and bias errors, the system and measurement equations are

$$\begin{aligned}
\dot{\boldsymbol{\varepsilon}} &= -\boldsymbol{\omega}^\times\boldsymbol{\varepsilon} + \frac{\boldsymbol{b}_\omega}{2} + \boldsymbol{w}_\omega, \\
\dot{\boldsymbol{b}}_\omega &= \boldsymbol{w}_b, \\
\boldsymbol{y} &= \boldsymbol{\varepsilon} + \boldsymbol{v}_p,
\end{aligned} \tag{11}$$

so that in the notation of (1) and (2),

$$\mathbf{A} = \begin{bmatrix} -\boldsymbol{\omega}^\times & \frac{1}{2}\mathbf{I} \\ \mathbf{0} & \mathbf{0} \end{bmatrix}, \quad \mathbf{H} = \begin{bmatrix} \mathbf{I} & \mathbf{0} \end{bmatrix}. \tag{12}$$

In [8], two filter implementations are considered, labeled cases (a) and (b) (for details please refer to [8]). Both of these cases are covered by (11), since case (b) can be obtained by setting $\boldsymbol{\omega} \equiv \boldsymbol{0}$ (see [8]). To find the state-transition matrix, it is necessary to solve the undisturbed system

$$\begin{aligned}
\dot{\boldsymbol{\varepsilon}} &= -\boldsymbol{\omega}^\times\boldsymbol{\varepsilon} + \frac{\boldsymbol{b}_\omega}{2}, \quad \boldsymbol{\varepsilon}(0) = \boldsymbol{\varepsilon}_0 \\
\dot{\boldsymbol{b}}_\omega &= \boldsymbol{0}, \quad \boldsymbol{b}_\omega(0) = \boldsymbol{b}_{\omega 0}
\end{aligned} \tag{13}$$

For the general case of time-varying angular velocities $\boldsymbol{\omega}(t)$, it is not possible to obtain a closed-form solution for the state-transition matrix corresponding to (13). This situation can be dealt with using the filter implementation of case (b), in which case the term containing $\boldsymbol{\omega}(t)$ in (13) disappears. However, as shown in [8], the implementation of case (b) is more sensitive to measurement noise than case (a), and it is desirable to implement the filter in the form of case (a) if possible. For many space missions, the satellite angular velocity is either approximately constant or very small or both (for example, inertially fixed, earth-pointing, spin-stabilized spacecraft). For very small angular velocities, it is reasonable to set $\boldsymbol{\omega} = \boldsymbol{0}$ in (13) and use the resulting gains. However, in order to cover the case of spin-stabilized satellites when $\boldsymbol{\omega}$ cannot be neglected, approximate gains are derived for the case of non-zero constant angular velocity. The case of $\boldsymbol{\omega} = \boldsymbol{0}$ will be recovered at the end as a special case.

Returning to the solution of (13), one obtains $\boldsymbol{b}_\omega(t) = \boldsymbol{b}_{\omega 0}$ so that

$$\dot{\boldsymbol{\varepsilon}} = -\boldsymbol{\omega}^\times\boldsymbol{\varepsilon} + \frac{\boldsymbol{b}_{\omega 0}}{2} \tag{14}$$

Thus, the state-transition matrix for the system $\dot{\boldsymbol{\varepsilon}} = -\boldsymbol{\omega}^\times\boldsymbol{\varepsilon}$ must be found. By uniqueness of the state-transition matrix, this is simply the rotation matrix satisfying

$$\dot{\mathbf{C}} = -\boldsymbol{\omega}^\times\mathbf{C}, \quad \mathbf{C}(0) = \mathbf{I}\,. \tag{15}$$

Now, pre-multiplying (14) by $\mathbf{C}^T$, it is obtained that

$$\mathbf{C}^T\dot{\boldsymbol{\varepsilon}}+\mathbf{C}^T\boldsymbol{\omega}^{\times}\boldsymbol{\varepsilon}=\mathbf{C}^T\,\frac{\boldsymbol{b}_{\omega 0}}{2}\,, \tag{16}$$

which leads to

$$\frac{d}{dt}\left(\mathbf{C}^T\boldsymbol{\varepsilon}\right)=\mathbf{C}^T\,\frac{\boldsymbol{b}_{\omega 0}}{2}\,. \tag{17}$$

Integrating this leads to the solution for $\boldsymbol{\varepsilon}$, given by

$$\boldsymbol{\varepsilon}(t)=\mathbf{C}(t)\boldsymbol{\varepsilon}_0+\frac{1}{2}\mathbf{C}(t)\int_0^t\mathbf{C}^T(\tau)d\tau\boldsymbol{b}_{\omega 0}\,. \tag{18}$$

Combining the above results, the state-transition matrix is assembled to be

$$\boldsymbol{\Phi}(t)=\begin{bmatrix}\mathbf{C}(t) & \frac{1}{2}\mathbf{C}(t)\int_0^t\mathbf{C}^T(\tau)d\tau\\ \mathbf{0} & \mathbf{I}\end{bmatrix}. \tag{19}$$

It is assumed that the initial error covariance is given by

$$\mathbf{P}_0=diag\left\{\sigma_1\quad\sigma_1\quad\sigma_1\quad\sigma_2\quad\sigma_2\quad\sigma_2\right\}, \tag{20}$$

and that the measurement noise covariance is given by

$$\mathbf{R}=r\mathbf{I}\,. \tag{21}$$

Remark: In practice, the initial error and measurement noise covariances will not have the form of (20) and (21). This simplification is made to allow the analysis to proceed, and yield a simple closed form solution for the transient gain approximation. As shown in [17, p.258], provided the initial error, measurement and process noise covariances upper bound the true covariances in a full Kalman filter implementation, then the computed error covariance will upper bound the actual error covariance for all time. Therefore, approximations (20) and (21) should upper bound the true initial error and measurement noise covariances.

It is assumed that the angular velocity vector is given by

$$\boldsymbol{\omega}=\omega_0\boldsymbol{a}\,, \tag{22}$$

where ω_0 is a constant scalar, and $\boldsymbol{a}$ is a constant unit vector. The associated rotation matrix is [13, p. 30]

$$\mathbf{C}=\cos(\omega_0 t)\mathbf{I}+\left(1-\cos(\omega_0 t)\right)\boldsymbol{a}\boldsymbol{a}^T-\sin(\omega_0 t)\boldsymbol{a}^{\times}\,. \tag{23}$$

From this, one has

$$\int_0^t\mathbf{C}(\tau)d\tau=\frac{\sin(\omega_0 t)}{\omega_0}\mathbf{I}+\left(t-\frac{\sin(\omega_0 t)}{\omega_0}\right)\boldsymbol{a}\boldsymbol{a}^T+\frac{\cos(\omega_0 t)-1}{\omega_0}\boldsymbol{a}^{\times}\,. \tag{24}$$

Making use of the identity $\boldsymbol{a}^{\times}\boldsymbol{a}^{\times} = \boldsymbol{a}\boldsymbol{a}^{T} - \mathbf{I}$, it can be shown by direct multiplication from (23) and (24) that

$$\mathbf{C}(t)\int_0^t \mathbf{C}^T(\tau)d\tau = \int_0^t \mathbf{C}(\tau)d\tau\,. \tag{25}$$

Hence, the state-transition matrix is given by

$$\mathbf{\Phi}(t) = \begin{bmatrix} \mathbf{C}(t) & \frac{1}{2}\int_0^t \mathbf{C}(\tau)d\tau \\ \mathbf{0} & \mathbf{I} \end{bmatrix} \tag{26}$$

and hence, the integrand in the covariance expression (eq. (9)) is given by

$$\frac{\mathbf{\Phi}^T(t)\mathbf{H}^T\mathbf{H}\mathbf{\Phi}(t)}{r} = \begin{bmatrix} \mathbf{C}(t)^T\mathbf{C}(t) & \frac{\mathbf{C}^T(t)}{2}\int_0^t \mathbf{C}(\tau)d\tau \\ \int_0^t \mathbf{C}^T(\tau)d\tau\frac{\mathbf{C}(t)}{2} & \frac{1}{4}\int_0^t \mathbf{C}^T(\tau)d\tau\int_0^t \mathbf{C}(\tau)d\tau \end{bmatrix}. \tag{27}$$

The following simplifications can be made

$$\begin{aligned} &\mathbf{C}^T\mathbf{C} = \mathbf{I}, \\ &\mathbf{C}^T(t)\int_0^t \mathbf{C}(\tau)d\tau = \mathbf{C}^T(t)\mathbf{C}(t)\int_0^t \mathbf{C}^T(\tau)d\tau = \int_0^t \mathbf{C}^T(\tau)d\tau. \end{aligned} \tag{28}$$

Using (24), it is obtained that

$$\int_0^t \mathbf{C}^T(\tau)d\tau\int_0^t \mathbf{C}(\tau)d\tau = 2\frac{1-\cos(\omega_0 t)}{\omega_0^2}\mathbf{I} + \left(t^2 - 2\frac{1-\cos(\omega_0 t)}{\omega_0^2}\right)\boldsymbol{a}\boldsymbol{a}^T. \tag{29}$$

Therefore, (27) becomes

$$\frac{\mathbf{\Phi}^T(t)\mathbf{H}^T\mathbf{H}\mathbf{\Phi}(t)}{r} = \begin{bmatrix} \mathbf{I} & \frac{1}{2}\mathbf{A}(t) \\ \frac{1}{2}\mathbf{A}^T(t) & \frac{1}{4}\mathbf{B}(t) \end{bmatrix} \tag{30}$$

where

$$\begin{aligned} \mathbf{A}(t) &= \frac{\sin(\omega_0 t)}{\omega_0}\mathbf{I} + \left(t - \frac{\sin(\omega_0 t)}{\omega_0}\right)\boldsymbol{a}\boldsymbol{a}^T - \frac{\cos(\omega_0 t)-1}{\omega_0}\boldsymbol{a}^{\times}, \\ \mathbf{B}(t) &= 2\frac{1-\cos(\omega_0 t)}{\omega_0^2}\mathbf{I} + \left(t^2 - 2\frac{1-\cos(\omega_0 t)}{\omega_0^2}\right)\boldsymbol{a}\boldsymbol{a}^T. \end{aligned} \tag{31}$$

These expressions are readily integrated to give

$$
\begin{aligned}
\int_0^t \mathbf{A}(\tau)d\tau &= \frac{1-\cos(\omega_0 t)}{\omega_0^2}\mathbf{I} + \left(\frac{t^2}{2} - \frac{1-\cos(\omega_0 t)}{\omega_0^2}\right)\boldsymbol{a}\boldsymbol{a}^T \\
&\quad - \left(\frac{\sin(\omega_0 t)}{\omega_0^2} - \frac{t}{\omega_0}\right)\boldsymbol{a}^{\times}, \\
\int_0^t \mathbf{B}(\tau)d\tau &= 2\left(\frac{t}{\omega_0^2} - \frac{\sin(\omega_0 t)}{\omega_0^3}\right)\mathbf{I} \\
&\quad + \left(\frac{t^3}{3} - 2\left(\frac{t}{\omega_0^2} - \frac{\sin(\omega_0 t)}{\omega_0^3}\right)\right)\boldsymbol{a}\boldsymbol{a}^T.
\end{aligned} \tag{32}
$$

This leads to the expression to be inverted in (9),

$$
\mathbf{P}_0^{-1} + \frac{1}{r}\int_0^t \mathbf{\Phi}^T(\tau)\mathbf{H}^T\mathbf{H}\mathbf{\Phi}(\tau)d\tau = \begin{bmatrix} \mathbf{D} & \mathbf{E} \\ \mathbf{E}^T & \mathbf{F} \end{bmatrix}, \tag{33}
$$

where

$$
\begin{aligned}
\mathbf{D} &= \left(\frac{t}{r} + \frac{1}{\sigma_1}\right)\mathbf{I}, \\
\mathbf{E} &= \frac{1-\cos(\omega_0 t)}{2\omega_0^2 r}\mathbf{I} + \left(\frac{t^2}{4r} - \frac{1-\cos(\omega_0 t)}{2\omega_0^2 r}\right)\boldsymbol{a}\boldsymbol{a}^T - \left(\frac{\sin(\omega_0 t)}{2\omega_0^2 r} - \frac{t}{2\omega_0 r}\right)\boldsymbol{a}^{\times}, \\
\mathbf{F} &= \left(\frac{1}{\sigma_2} + \frac{t}{2\omega_0^2 r} - \frac{\sin(\omega_0 t)}{2\omega_0^3 r}\right)\mathbf{I} + \left(\frac{t^3}{12r} - \left(\frac{t}{2\omega_0^2 r} - \frac{\sin(\omega_0 t)}{2\omega_0^3 r}\right)\right)\boldsymbol{a}\boldsymbol{a}^T.
\end{aligned} \tag{34}
$$

By the matrix inversion lemma [18, p. 23], one has

$$
\begin{bmatrix} \mathbf{D} & \mathbf{E} \\ \mathbf{E}^T & \mathbf{F} \end{bmatrix}^{-1} = \begin{bmatrix} \mathbf{D}^{-1} + \mathbf{D}^{-1}\mathbf{E}\left(\mathbf{F} - \mathbf{E}^T\mathbf{D}^{-1}\mathbf{E}\right)^{-1}\mathbf{E}^T\mathbf{D}^{-1} & -\mathbf{D}^{-1}\mathbf{E}\left(\mathbf{F} - \mathbf{E}^T\mathbf{D}^{-1}\mathbf{E}\right)^{-1} \\ -\left(\mathbf{F} - \mathbf{E}^T\mathbf{D}^{-1}\mathbf{E}\right)^{-1}\mathbf{E}^T\mathbf{D}^{-1} & \left(\mathbf{F} - \mathbf{E}^T\mathbf{D}^{-1}\mathbf{E}\right)^{-1} \end{bmatrix}. \tag{35}
$$

Therefore, the inverses $\mathbf{D}^{-1}$ and $\left(\mathbf{F} - \mathbf{E}^T\mathbf{D}^{-1}\mathbf{E}\right)^{-1}$ are needed. To proceed, the following lemma is needed.

Lemma 1 Given an arbitrary unit vector $\boldsymbol{a}$, and scalar values $b,\ c,\ d$, the matrix

$$
X = b\mathbf{I} + c\boldsymbol{a}\boldsymbol{a}^T + d\boldsymbol{a}^{\times} \tag{36}
$$

is invertible if and only if the matrix

$$
\mathbf{Y} = \begin{bmatrix} b & 0 & -d \\ c & b+c & d \\ d & 0 & b \end{bmatrix} \tag{37}
$$

is invertible, and when it is invertible, the inverse is given by

$$
\mathbf{X}^{-1} = \frac{b}{b^2+d^2}\mathbf{I} + \frac{d^2 - bc}{\left(b^2+d^2\right)\left(b+c\right)}\boldsymbol{a}\boldsymbol{a}^T - \frac{d}{b^2+d^2}\boldsymbol{a}^{\times}. \tag{38}
$$

Proof: Contained in the appendix.

Using the Lemma 1 together with (35), the approximate covariance in (9) can be solved for, and an exact analytical expression for the Kalman gains may be computed. Omitting the much tedious algebra, the final expressions are derived as

$$
\begin{aligned}
\hat{\mathbf{K}} &= \begin{bmatrix} \hat{\mathbf{K}}_p \\ \hat{\mathbf{K}}_b \end{bmatrix}, \\
\hat{\mathbf{K}}_p &= \hat{k}_{p1}\mathbf{I} + \left(\hat{k}_{p2} - \hat{k}_{p1}\right)\boldsymbol{a}\boldsymbol{a}^T, \\
\hat{\mathbf{K}}_b &= \hat{k}_{b1}\mathbf{I} + \left(\hat{k}_{b2} - \hat{k}_{b1}\right)\boldsymbol{a}\boldsymbol{a}^T + \hat{k}_{b3}\boldsymbol{a}^{\times}.
\end{aligned}
\tag{39}
$$

where

$$
\begin{aligned}
\hat{k}_{p1} &= \frac{t2\omega_0^2\sigma_1\sigma_2 - \sin(\omega_0 t)2\omega_0\sigma_1\sigma_2 - \cos(\omega_0 t)2\omega_0^2\sigma_2 r + 2\omega_0^2\sigma_2 r + 4\omega_0^4\sigma_1 r}{d_2}, \\
\hat{k}_{p2} &= \frac{t^3 4\sigma_1\sigma_2 + t^2 12\sigma_2 r + 48\sigma_1 r}{d_1}, \\
\hat{k}_{b1} &= \frac{\sin(\omega_0 t)2\omega_0^3\sigma_2 r - \cos(\omega_0 t)2\omega_0^2\sigma_1\sigma_2 + 2\omega_0^2\sigma_1\sigma_2}{d_2}, \\
\hat{k}_{b2} &= \frac{t^2 12\sigma_1\sigma_2 + t24\sigma_2 r}{d_1}, \\
\hat{k}_{b3} &= \frac{t2\omega_0^3\sigma_1\sigma_2 - \sin(\omega_0 t)2\omega_0^2\sigma_1\sigma_2 - \cos(\omega_0 t)2\omega_0^3\sigma_2 r + 2\omega_0^3\sigma_2 r}{d_2},
\end{aligned}
\tag{40}
$$

and

$$
\begin{aligned}
d_1 &= t^4\sigma_1\sigma_2 + t^3 4\sigma_2 r + t48\sigma_1 r + 48r^2, \\
d_2 &= t^2\sigma_1\sigma_2\omega_0^2 + t\left(4\omega_0^4\sigma_1 r + 2\omega_0^2\sigma_2 r\right) + \cos(\omega_0 t)2\sigma_1\sigma_2 - \sin(\omega_0 t)2\omega_0\sigma_2 r + 4\omega_0^4 r^2 - 2\sigma_1\sigma_2.
\end{aligned}
\tag{41}
$$

It will be useful to examine the gains when the angular velocity is constant about one of the spacecraft principal axes. Consider a constant rotation rate ω_0 about the spacecraft *x*-axis. In this case, the angular velocity is given by $\boldsymbol{\omega} = \begin{bmatrix}\omega_0 & 0 & 0\end{bmatrix}^T$, and the gains are given by

$$
\hat{\mathbf{K}}(t) = \begin{bmatrix}
\hat{k}_{p2} & 0 & 0 \\
0 & \hat{k}_{p1} & 0 \\
0 & 0 & \hat{k}_{p1} \\
\hat{k}_{b2} & 0 & 0 \\
0 & \hat{k}_{b1} & -\hat{k}_{b3} \\
0 & \hat{k}_{b3} & \hat{k}_{b1}
\end{bmatrix}.
\tag{42}
$$

It is worth examining this case in more detail in order to obtain suitable times to switch from transient to steady-state filter operation. In this case, the system (11) with initial error and measurement noise covariances given by (20) and (21) decouple into two subsystems of the form

$$\mathbf{\Phi}_1(t) = \begin{bmatrix} 1 & \dfrac{t}{2} \\ 0 & 1 \end{bmatrix},\ \mathbf{H}_1 = \begin{bmatrix} 1 & 0 \end{bmatrix}, \quad , \qquad \mathbf{P}_{01} = \begin{bmatrix} \sigma_1 & 0 \\ 0 & \sigma_2 \end{bmatrix},\ \mathbf{R} = r \tag{43}$$

and

$$\mathbf{\Phi}_2(t) = \begin{bmatrix} \cos(\omega_0 t) & \sin(\omega_0 t) & \dfrac{\sin(\omega_0 t)}{\omega_0} & \dfrac{1-\cos(\omega_0 t)}{\omega_0} \\ -\sin(\omega_0 t) & \cos(\omega_0 t) & \dfrac{\cos(\omega_0 t)-1}{\omega_0} & \dfrac{\sin(\omega_0 t)}{\omega_0} \\ 0 & 0 & 1 & 0 \\ 0 & 0 & 0 & 1 \end{bmatrix},$$
$$\mathbf{H}_2 = \begin{bmatrix} 1 & 0 & 0 & 0 \\ 0 & 1 & 0 & 0 \end{bmatrix},\ \mathbf{P}_{02} = \begin{bmatrix} \sigma_1 & 0 & 0 & 0 \\ 0 & \sigma_1 & 0 & 0 \\ 0 & 0 & \sigma_2 & 0 \\ 0 & 0 & 0 & \sigma_2 \end{bmatrix},\ \mathbf{R}_2 = \begin{bmatrix} r & 0 \\ 0 & r \end{bmatrix} \tag{44}$$

Subsystems (43) and (44) have the associated approximate transient Kalman gains given by

$$\begin{aligned} \mathbf{K}_1(t) &= \mathbf{P}_1(t)\mathbf{H}_1^T(t)\mathbf{R}_1^{-1}, \\ \mathbf{K}_2(t) &= \mathbf{P}_2(t)\mathbf{H}_2^T(t)\mathbf{R}_2^{-1}, \end{aligned} \tag{45}$$

where

$$\begin{aligned} \mathbf{P}_1(t) &= \mathbf{\Phi}_1(t)\left(\mathbf{P}_{01}^{-1} + \int_0^t \mathbf{\Phi}_1^T(\tau)\mathbf{H}_1^T\mathbf{R}_1^{-1}\mathbf{H}_1\mathbf{\Phi}_1(\tau)d\tau\right)^{-1}\mathbf{\Phi}_1^T(t), \\ \mathbf{P}_2(t) &= \mathbf{\Phi}_2(t)\left(\mathbf{P}_{02}^{-1} + \int_0^t \mathbf{\Phi}_2^T(\tau)\mathbf{H}_2^T\mathbf{R}_2^{-1}\mathbf{H}_2\mathbf{\Phi}_2(\tau)d\tau\right)^{-1}\mathbf{\Phi}_2^T(t). \end{aligned} \tag{46}$$

Clearly, the covariances in (46) are initially dominated by the initial error variance, and later dominated by the integral terms. The time of this switch in dominance can be estimated for each state component from the diagonal terms by the equality

$$\begin{aligned} \left\{\int_0^{t_{i1}} \mathbf{\Phi}_1^T(\tau)\mathbf{H}_1^T\mathbf{R}_1^{-1}\mathbf{H}_1\mathbf{\Phi}_1(\tau)d\tau\right\}_{ii} &= \chi\left\{\mathbf{P}_{01}^{-1}\right\}_{ii},\ i=1,2, \\ \left\{\int_0^{t_{i2}} \mathbf{\Phi}_2^T(\tau)\mathbf{H}_2^T\mathbf{R}_2^{-1}\mathbf{H}_2\mathbf{\Phi}_2(\tau)d\tau\right\}_{ii} &= \chi\left\{\mathbf{P}_{02}^{-1}\right\}_{ii},\ i=1,3, \end{aligned} \tag{47}$$

where $\chi \gg 1$ is a large positive number and a design parameter. Physically, these times represent the beginning of unbiased estimation, after which the estimation error is determined by measurement noise, and practically does not depend on the initial indeterminacy of the system [16]. The time $t^* = \max(t_{i1}, t_{i2})$ is a suitable time to switch the filter from transient to steady-state operation.

The integrals in (47) are evaluated to be

$$\int_0^t \mathbf{\Phi}_1^T(\tau)\mathbf{H}_1^T\mathbf{R}_1^{-1}\mathbf{H}_1\mathbf{\Phi}_1(\tau)d\tau = \begin{bmatrix} \frac{t}{r} & \frac{t^2}{4r} \\ \frac{t^2}{4r} & \frac{t^3}{12r} \end{bmatrix} \tag{48}$$

and

$$\int_0^t \mathbf{\Phi}_2^T(\tau)\mathbf{H}_2^T\mathbf{R}_2^{-1}\mathbf{H}_2\mathbf{\Phi}_2(\tau)d\tau = \begin{bmatrix} \frac{t}{r} & 0 & \frac{1-\cos(\omega_0 t)}{2\omega_0^2 r} & \frac{\sin(\omega_0 t)}{2\omega_0^2 r} - \frac{t}{2\omega_0 r} \\ 0 & \frac{t}{r} & \frac{t}{2\omega_0 r} - \frac{\sin(\omega_0 t)}{2\omega_0^2 r} & \frac{1-\cos(\omega_0 t)}{2\omega_0^2 r} \\ \frac{1-\cos(\omega_0 t)}{2\omega_0^2 r} & \frac{t}{2\omega_0 r} - \frac{\sin(\omega_0 t)}{2\omega_0^2 r} & \frac{t}{2\omega_0^2 r} - \frac{\sin(\omega_0 t)}{2\omega_0^3 r} & 0 \\ \frac{\sin(\omega_0 t)}{2\omega_0^2 r} - \frac{t}{2\omega_0 r} & \frac{1-\cos(\omega_0 t)}{2\omega_0^2 r} & 0 & \frac{t}{2\omega_0^2 r} - \frac{\sin(\omega_0 t)}{2\omega_0^3 r} \end{bmatrix}. \tag{49}$$

Therefore, from (47), (48) and (49) the switch times are obtained from the expressions

$$\begin{aligned} t_{11} = t_{12} &= \min\left\{ t : \frac{t}{r} \geq \frac{\chi}{\sigma_1} \right\}, \\ t_{21} &= \min\left\{ t : \frac{t^3}{12r} \geq \frac{\chi}{\sigma_2} \right\}, \\ t_{32} &= \min\left\{ t : \frac{t}{2\omega_0^2 r} - \frac{\sin(\omega_0 t)}{2\omega_0^3 r} \geq \frac{\chi}{\sigma_2} \right\}. \end{aligned} \tag{50}$$

The third switch time may be approximated by

$$t_{32} = \min\left\{ t : \frac{t}{2\omega_0^2 r} \geq \frac{\chi}{\sigma_2} + \frac{1}{2\omega_0^3 r} \right\}. \tag{51}$$

Finally, from (50) and (51) the switch times can be solved for by

$$\begin{aligned} t_{11} = t_{12} &= \frac{\chi r}{\sigma_1}, \\ t_{21} &= \left(\frac{12\chi r}{\sigma_2} \right)^{\frac{1}{3}}, \\ t_{32} &= \frac{2\chi\omega_0^2 r}{\sigma_2} + \frac{1}{\omega_0}. \end{aligned} \tag{52}$$

A suitable time to switch from transient to steady-state operation is given by

$$t^* = \max(t_{11}, t_{21}, t_{32}). \tag{53}$$

Slowly Spinning Spacecraft

This is a very important case, since in many cases, satellites do not have large angular velocities. In the case of zero angular velocity $\omega_0 = 0$, the system decouples into three identical subsystems given by (43). Using the gain obtained for that subsystem, the gain for the full system is given by

$$\hat{\mathbf{K}}(t)=\begin{bmatrix}\hat{k}_{p2} & 0 & 0\\ 0 & \hat{k}_{p2} & 0\\ 0 & 0 & \hat{k}_{p2}\\ \hat{k}_{b2} & 0 & 0\\ 0 & \hat{k}_{b2} & 0\\ 0 & 0 & \hat{k}_{b2}\end{bmatrix}. \qquad (54)$$

From (52), we have that a suitable time to switch from transient to steady-state filter operation is

$$t^* = \frac{\chi r}{\sigma_1}, \qquad (55)$$

where $\chi >> 1$ is a designer chosen parameter.

By successive application of L'Hôpital's theorem, it can be shown that $\hat{k}_{p1} \to \hat{k}_{p2}$, $\hat{k}_{b1} \to \hat{k}_{b2}$ and $\hat{k}_{b3} \to 0$ point-wise as $\omega_0 \to 0$. This is to be expected, and the implication of this is that for very slowly spinning spacecraft, the approximation (55) may be used with case (a). Since the error dynamics are independent of the spacecraft angular velocity in case (b), the approximation (54) is always used with case (b).

To summarize, if the initial attitude and gyro bias errors are known to be small, the following simple Kalman filter implementation may be used.

Summary of the Filter Algorithm with Transient Modification

Let the initial error and measurement noise covariances be given by (20) and (21). Compute the switching time, t^* from (53) or (55). The attitude estimate is obtained by numerical integration of

$$\dot{\hat{\boldsymbol{\alpha}}} = \mathbf{W}(\hat{\boldsymbol{\alpha}})\bar{\boldsymbol{\omega}},$$

$$\dot{\hat{\boldsymbol{b}}}_\omega = k_b \boldsymbol{\varepsilon}_{GM}\, sign(\eta_{GM}),$$

where

$$\bar{\boldsymbol{\omega}} = \begin{cases} \boldsymbol{\omega}^m - \hat{\boldsymbol{b}}_\omega - \mathbf{K}_p \boldsymbol{\varepsilon}_{GM}\, sign(\eta_{GM}), & case\ \ (a),\\ \delta\mathbf{C}^{GM}\left(\boldsymbol{\omega}^m - \hat{\boldsymbol{b}}_\omega - \mathbf{K}_p \boldsymbol{\varepsilon}_{GM}\, sign(\eta_{GM})\right), & case\ \ (b),\end{cases}$$

$(\boldsymbol{\varepsilon}_{GM}, \eta_{GM})$ is the quaternion parameterization of $\delta\mathbf{C}^{GM} = \hat{\mathbf{C}}_{bI}^{G}(\hat{\boldsymbol{\alpha}})\left(\hat{\mathbf{C}}_{bI}^{M}\right)^{-1}$ and

$$\mathbf{K}_p = \begin{cases} 2\hat{\mathbf{K}}_p & \text{from eq (46)}, \quad 0 \le t \le t^*,\\ k_p\mathbf{I} & \text{as in [8]}, \quad t > t^*,\end{cases}$$

$$\mathbf{K}_b = \begin{cases} \hat{\mathbf{K}}_b & \text{from eq (46)}, \quad 0 \le t \le t^*,\\ k_b\mathbf{I} & \text{as in [8]}. \quad t > t^*.\end{cases}$$

III. Numerical Example

A numerical example is now presented to demonstrate the effectiveness of the approach presented in the paper to recover the transient performance of a Kalman filter for the gyro-corrected attitude determination problem, while maintaining computational simplicity. Note that the details of the system (sensor noise, gyro bias, initial uncertainties) are the same as in [8], however the simulation scenarios are different. In this paper, two cases are considered with the satellite rotating about the body *x*-axis with angular rate 1 deg/s and 10 deg/s respectively.

In this section, the results in this paper are demonstrated, for two cases of a satellite rotating about the body *x*-axis at a rate of 1 deg/s and 10 deg/s respectively. MATLAB™ is used to perform the simulations. The attitude and gyro bias are given initial uncertainties

$$\sigma_1 = \sigma_2 = \left(\frac{\pi}{180}\right)^2 .$$

The gyro measurements are available at a 100 Hz sample rate, and are given by

$$\boldsymbol{\omega}^m = \boldsymbol{\omega} + \boldsymbol{b} + \boldsymbol{w}_\omega , \tag{56}$$

where $\boldsymbol{w}_\omega$ consists of random numbers uniformly-distributed in the range $\pm 0.05 \ \deg / s$ for each entry. The gyro bias is given by the constant vector

$$\boldsymbol{b} = \begin{bmatrix} 1 \\ -1 \\ 1 \end{bmatrix} \ \deg / s \tag{57}$$

The external attitude measurements have error

$$\delta \mathbf{C}^M = I + 2\left(\boldsymbol{v}_k^\times \boldsymbol{v}_k^\times - \left(1 - \boldsymbol{v}_k^T \boldsymbol{v}_k\right)^{\frac{1}{2}} \boldsymbol{v}_k^\times \right), \tag{58}$$

where $\boldsymbol{v}_k$ is a zero-mean Gaussian white noise sequence, with covariance $E\left\{\boldsymbol{v}_k \boldsymbol{v}_k^T\right\} = r_d \mathbf{I}$, and $r_d = \left(\frac{\pi}{180}\right)^2$. The process and measurement noise covariances are

$$\mathbf{R} = r_d \Delta T \mathbf{I}, \ \ \mathbf{Q} = \begin{bmatrix} \left(\frac{0.05\pi}{180}\right)^2 \mathbf{I} & 0 \\ 0 & 10^{-10}\mathbf{I} \end{bmatrix}, \tag{59}$$

where $\Delta T = 1$s.

As in [8], the steady-state Kalman gains are

$$\begin{aligned} k_p &= 6.9223 \times 10^{-2}, \\ k_b &= 5.7296 \times 10^{-4}. \end{aligned} \tag{60}$$

The parameterization chosen for the attitude estimate is the quaternion. Therefore, the filter equations become

$$\begin{aligned}
&\begin{bmatrix} \dot{\hat{\boldsymbol{q}}} \\ \dot{q}_4 \end{bmatrix} = \frac{1}{2}\begin{bmatrix} \hat{\boldsymbol{q}}^{\times} + q_4\mathbf{I} \\ -\boldsymbol{q}^T \end{bmatrix}\left(\boldsymbol{\omega}^m - \hat{\boldsymbol{b}} + \boldsymbol{u}_p\right),\ Case\ (a), \\
&\begin{bmatrix} \dot{\hat{\boldsymbol{q}}} \\ \dot{q}_4 \end{bmatrix} = \frac{1}{2}\begin{bmatrix} \hat{\boldsymbol{q}}^{\times} + q_4\mathbf{I} \\ -\boldsymbol{q}^T \end{bmatrix}\delta\mathbf{C}^{GM}(t_k)\left(\boldsymbol{\omega}^m - \hat{\boldsymbol{b}} + \boldsymbol{u}_p\right),\ Case\ (b), \\
&\dot{\hat{\boldsymbol{b}}} = -\boldsymbol{u}_b, \\
&\boldsymbol{u}_p(t) = -\mathbf{K}_p(t_k)\boldsymbol{y}(t_k),\ \ t_k \le t < t_{k+1}, \\
&\boldsymbol{u}_b(t) = -\mathbf{K}_b(t_k)\boldsymbol{y}(t_k),\ \ t_k \le t < t_{k+1}.
\end{aligned} \tag{61}$$

where

$$\boldsymbol{y} = \boldsymbol{\varepsilon}_{GM}\, sign(\eta_{GM}), \tag{62}$$

and $\left(\boldsymbol{\varepsilon}_{GM}, \eta_{GM}\right)$ is a quaternion parameterizing $\delta\mathbf{C}^{GM}$, and $\left(\mathbf{q}, q_4\right)$ is the quaternion parameterizing the attitude estimate.

The true initial attitude is $\begin{bmatrix} \boldsymbol{q}_0^T & q_{40} \end{bmatrix}^T = \begin{bmatrix} 0 & 0 & 0 & 1 \end{bmatrix}^T$. The initial attitude estimate error is given by $\boldsymbol{\varepsilon}_0 = \dfrac{\pi}{180}\begin{bmatrix} 1 & 1 & -1 \end{bmatrix}^T$ with $sign(\eta_0) = 1$, and the initial gyro bias estimate is $\hat{\boldsymbol{b}}_0 = \begin{bmatrix} 0 & 0 & 0 \end{bmatrix}^T$ deg/s.

For the simulation of a 1 degree/second spin rate, the same transient approximations to the Kalman gain are used for both cases (a) and (b) (those corresponding to , $\boldsymbol{\omega} \equiv \boldsymbol{0}$, given by (54)). For the simulation of a 10 degree/second spin rate, case (a) uses the transient approximation given by (42). For this example, $\chi = 100$ has been chosen, resulting in switch times $t_{11} = 100$ seconds, $t_{21} = 10.6$ seconds for both spin rates, and $t_{32} = 57.3$ seconds in the case of a 1 degree/second spin rate and $t_{32} = 11.8$ seconds in the case of a 10 degree/second spin rate. The transient approximations are therefore applied for 100 seconds, at which time they are switched to the constant gains given by (60).

It is of interest to examine the closed-loop eigenvalues of the steady-state error dynamics with the gains (60). For case (b), these are the same no matter what the satellite spin rate, and are $-0.0209, -0.0137$ each of multiplicity three, for which the slowest mode takes 50.6 seconds to decay by 50%. For case (a), the closed-loop eigenvalues depend upon the satellite spin rate, and are given by $-0.0209, -0.0137, -0.0284 \pm 0.0224j, -0.0062 \pm 0.0049j$ for a spin rate of 1 degree/second (for which the slowest mode takes 111.8 seconds to decay by 50%), and $-0.0209, -0.0137, -0.0343 \pm 0.1761j, -0.0003 \pm 0.0016j$ for a spin rate of 10 degree/second (for which the slowest mode takes 2310.5 seconds to decay by 50%). This illustrates two key points. First, case (b) has the advantage that the closed-loop eigenvalues are always the same, and therefore the convergence rate stays the same. Second, it illustrates in particular for case (a) the need for a transient approximation to the Kalman gain, since the decay times can become very long for a non-zero spin rate.

Figures 1 and 2 show the time histories of the attitude estimation errors and the gyro bias estimates for both simulations. From these figures it can be seen that with the addition of the transient approximation to the Kalman gain, both cases (a) and (b) have very similar convergence, which is much faster than the decay times corresponding to the closed-loop eigenvalues above for both cases (a) and (b). Thus, the transient performance has been significantly improved with the addition of the approximate Kalman transient gains. Note from the figures that as shown in [8], the implementation of case (b) is much more sensitive to measurement noise than case (a), in particular for larger angular velocities.

A second set of simulations was performed to examine the filter performance when the initial estimation errors do not match the initial uncertainty covariances σ_1 and σ_2. This set of simulations consists of three separate scenarios. All parameters are kept the same as in the simulations for a 1 degree/second spin-rate (in particular the filter parameters are kept the same), except the initial attitude estimate error takes the values $\boldsymbol{\varepsilon}_0 = 0.1\times\frac{\pi}{180}\begin{bmatrix}1 & 1 & -1\end{bmatrix}^T$, $\boldsymbol{\varepsilon}_0 = \frac{\pi}{180}\begin{bmatrix}1 & 1 & -1\end{bmatrix}^T$ and $\boldsymbol{\varepsilon}_0 = 10\times\frac{\pi}{180}\begin{bmatrix}1 & 1 & -1\end{bmatrix}^T$ and the true gyro bias takes the values $\boldsymbol{b} = 0.1\times\begin{bmatrix}1 & -1 & 1\end{bmatrix}$ deg$/s$, $\boldsymbol{b} = \begin{bmatrix}1 & -1 & 1\end{bmatrix}$ deg$/s$ and $\boldsymbol{b} = 10\times\begin{bmatrix}1 & -1 & 1\end{bmatrix}$ deg$/s$ respectively for the three scenarios. Therefore, the initial estimate errors are one tenth, the same and ten times the original estimate errors respectively. Figure 3 shows the resulting estimation errors for case (a) and Figure 4 shows the resulting estimation errors for case (b). From these figures it can be seen that both cases (a) and (b) exhibit similar performance, and that the filters exhibit rapid convergence even though the initial estimate error is quite different from the designed for initial uncertainties (reflected by the covariances σ_1 and σ_2).

A third set of simulations was performed to examine the filter performance when the measurement noise has different covariance compared to what the filter is tuned for. This set of simulations consists of three separate scenarios. All parameters are kept the same as in the simulations for a 1 degree/second spin-rate (in particular, the filter parameters are kept the same), except the attitude measurement noise covariance is given by $r_d = \left(0.1\times\frac{\pi}{180}\right)^2$, $r_d = \left(\frac{\pi}{180}\right)^2$ and $r_d = \left(10\times\frac{\pi}{180}\right)^2$ respectively for the three scenarios. Figure 5 shows the resulting estimation errors for case (a) and Figure 6 shows the resulting estimation errors for case (b). From these figures it can be seen that both cases (a) and (b) exhibit similar performance. As expected, the steady-state estimation errors vary significantly between the different scenarios. However, in all three scenarios, the filter convergence is still quite rapid.

IV. Conclusion

In conclusion, a previously presented simple Kalman filter implementation for the gyro corrected attitude determination problem has been extended to improve transient performance. The resulting filter is divided into two approximate parts, a transient part and a steady-state part. The transient addition to the filter is the main contribution of this paper. In the transient part, a time-varying Kalman gain approximation is used, while in the steady-state part, the Kalman gain is approximated as constant. It has been shown in a previous paper that using only the constant steady-state gain leads to global stability and close-to-optimal steady-state performance. However, as demonstrated in this paper, this can be at the expense of lost transient performance, leading to longer convergence times (compared to the Kalman filter). Therefore, this paper has presented simple analytical expressions approximating the transient part of the Kalman gain. A suitable time for switching from transient to steady-state filter operation has also been derived. As demonstrated with a numerical example, great gains in transient performance (faster convergence) may be made by initially implementing the time-varying transient approximation to the Kalman gain for a predetermined fixed period of time.

V. Acknowledgements

The author gratefully acknowledges the valuable discussions and feedback from James Lee, Yuri Kim and Alfred Ng of the Canadian Space Agency. The author also thanks the anonymous reviewers for their valuable suggestions which have helped to improve this paper.

VI. Appendix

Proof of Lemma 1: Let the unit vector be given by $\boldsymbol{a} = \mathbf{C}\boldsymbol{e}_1$, where $\mathbf{C}$ is some rotation matrix rotating the vector $\boldsymbol{e}_1 = \begin{bmatrix}1 & 0 & 0\end{bmatrix}^T$ onto $\boldsymbol{a}$ (this can always be done). Then,

$$\det(\mathbf{X}) = \det\left(\mathbf{C}\left(b\mathbf{I} + c\boldsymbol{e}_1\boldsymbol{e}_1^T + d\boldsymbol{e}_1^\times\right)\mathbf{C}^T\right) = \det(\mathbf{C})\det\left(b\mathbf{I} + c\boldsymbol{e}_1\boldsymbol{e}_1^T + d\boldsymbol{e}_1^\times\right)\det\left(\mathbf{C}^T\right) = \det\left(b\mathbf{I} + c\boldsymbol{e}_1\boldsymbol{e}_1^T + d\boldsymbol{e}_1^\times\right). \quad \textbf{(63)}$$

But,

$$b\mathbf{I} + c\boldsymbol{e}_1\boldsymbol{e}_1^T + d\boldsymbol{e}_1^\times = \begin{bmatrix} b+c & 0 & 0 \\ 0 & b & -d \\ 0 & d & b \end{bmatrix}, \quad \textbf{(64)}$$

and $\det\left(b\mathbf{I} + c\boldsymbol{e}_1\boldsymbol{e}_1^T + d\boldsymbol{e}_1^\times\right) = \left(b^2 + d^2\right)(b+c)$. It can readily be calculated that $\det(\mathbf{Y}) = \left(b^2 + d^2\right)(b+c)$ also. Therefore, since $\det(\mathbf{X}) = \det(\mathbf{Y})$, $\mathbf{X}$ is invertible if and only if $\mathbf{Y}$ is invertible. Now, assume that $\mathbf{X}$ is invertible. It is postulated that the inverse of $\mathbf{X}$ has the form

$$\mathbf{Z} = e\mathbf{I} + f\boldsymbol{a}\boldsymbol{a}^T + g\boldsymbol{a}^\times. \quad \textbf{(65)}$$

Then, it is required that

$$\mathbf{I} = \mathbf{XZ} = \left(be - dg\right)\mathbf{I} + \left(bf + ce + cf + dg\right)\boldsymbol{a}\boldsymbol{a}^T + \left(bg + de\right)\boldsymbol{a}^\times , \tag{66}$$

which implies that

$$\begin{bmatrix} b & 0 & -d \\ c & b+c & d \\ d & 0 & b \end{bmatrix}\begin{bmatrix} e \\ f \\ g \end{bmatrix} = \begin{bmatrix} 1 \\ 0 \\ 0 \end{bmatrix}, \tag{67}$$

but, this is solvable if and only if $\mathbf{Y}$, and hence $\mathbf{X}$ is invertible. Thus, by uniqueness of the inverse, the inverse is given by $\mathbf{Z}$, and is obtained by solving the above equation, which has the solution

$$e = \frac{b}{b^2 + d^2},\ f = \frac{d^2 - bc}{\left(b^2 + d^2\right)\left(b + c\right)},\ g = \frac{-d}{b^2 + d^2}. \tag{68}$$

This concludes the proof.

References

[1] Kim, Y., De Ruiter, A., Lee, J., Ng, A., "Robust Implementation of Kalman Filter for INS Correction", *Actual Problems of Aviation and Aerospace Systems: Processes, Models, Experiment,* No. 3 (25), vol. 12, 2007.

[2] E. J. Lefferts, F. L. Markley, M. D. Shuster, "Kalman Filtering for Spacecraft Attitude Determination," *AIAA Journal of Guidance and Control,* Vol. 5, No. 5, Sept.-Oct. 1982, pp. 417-429.

[3] J. L. Crassidis, F. L. Markley and Y. Cheng, “Survey of Nonlinear Attitude Estimation Methods”, *AIAA Journal of Guidance, Control and Dynamics*, vol. 30, No. 1, January-February 2007, pp. 12-28.

[4] A. Ng, K. Yoshihara, H. Hashimoto, L. Ngo-Phong, B. S. Kumar, A. de Ruiter, " Nanosatellite Mission For Demonstrating Formation Keeping Technology With Aerodynamic Drag," 11th International Space Conference of Pacific basin Societies (ISCOPS), Beijing, China, 16-18 May, 2007.

[5] J. Thienel and R. M. Sanner, “A Coupled Nonlinear Spacecraft Attitude Controller and Observer With an Unknown Constant Gyro Bias and Gyro Noise”, *IEEE Transactions on Automatic Control,* Vol. 48, No. 11, November 2003.

[6] J. K. Thienel and R. M. Sanner, “Hubble Space Telescope Angular Velocity Estimation During the Robotic Servicing Mission”, *AIAA Journal of Guidance, Control and Dynamics*, vol. 30, No. 1, January-February 2007, pp. 29-34.

[7] S. Salcudean, “A Globally Convergent Angular Velocity Observer for Rigid Body Motion”, *IEEE Transactions on Automatic Control*,, Vol. 36, No. 12, December 1991.

[8] A. de Ruiter, “A simple suboptimal Kalman filter implementation for a gyro-corrected satellite attitude determination system,” Proc. *IMechE Vol 224 (7) Part G: J. Aerospace Engineering*, 2010 pp. 787-802.

[9] J. R. Wertz, *Spacecraft Attitude Determination and Control*, Dordrecht, Holland: Kluwer Academic Publishers, 1978.

[10] M. D. Shuster and S. D. Oh, “Three-Axis Attitude Determination from Vector Observations”, *AIAA Journal of Guidance and Control*, Vol. 4, No. 1, Jan-Feb, 1981, pp. 70-77.

[11] Cohen, C.E., "Attitude Determination," *Global Positioning System: Theory and Applications,* Vol. II, edited by B. W. Parkinson and J. J. Spilker, Jr., AIAA, Washington, DC, 1996, pp. 519-538.

[12] M. D. Shuster, “A Survey of Attitude Representations”, *The Journal of the Astronautical Sciences*, Vol. 41, No. 4, Oct.-Dec. 1993, pp. 439-573.

[13] P. C. Hughes, *Spacecraft Attitude Dynamics*. New York: Dover Publications, 2004.

[14] R. L. Farrenkopf, "Analytic Steady-State Accuracy Solutions for Two Common Spacecraft Attitude Estimators", *AIAA Journal of Guidance and, Control*, vol. 1, No. 4, 1978, pp. 282-284.

[15] F. L. Markley, "Attitude Error Representations for Kalman Filtering," *AIAA Journal of Guidance, Control and Dynamics*, vol. 26, No. 2, March-April 2003, pp. 311-317.

[16] Y. Kim, *An Approach to Suboptimal Filtering in Applied Problems of Information Processing*, Scripta Technica, Inc, USA, 1990.

[17] A.H. Jazwinski,, *Stochastic Processes and Filtering Theory*, Academic Press, United Kingdom, 1970.

[18] K. Zhou with J. C. Doyle and K. Glover, *Robust and Optimal Control*, Prentice Hall, New Jersey, 1996.

Nomenclature

$\boldsymbol{a}$ = axis of rotation
$\mathbf{A}$ = system matrix
$\boldsymbol{b}_{\omega}$ = gyro measurement bias vector
$\hat{\boldsymbol{b}}_{\omega}$ = gyro measurement bias estimate
$\tilde{\boldsymbol{b}}_{\omega}$ = gyro measurement estimate error
$\mathbf{C}$ = rotation matrix
$\mathbf{C}_{bI}$ = rotation matrix representing the true spacecraft attitude
$\hat{\mathbf{C}}_{bI}^{M}$ = rotation matrix representing the external spacecraft attitude measurement
$\hat{\mathbf{C}}_{bI}^{G}$ = rotation matrix representing the gyro spacecraft attitude estimate
$\delta\mathbf{C}^{M}$ = rotation matrix representing the external attitude measurement error
$\delta\mathbf{C}^{G}$ = rotation matrix representing the true gyro attitude estimate error
$\delta\mathbf{C}^{GM}$ = rotation matrix representing the measured gyro attitude estimate error
$E\{\cdot\}$ = expectation operator
$\mathbf{H}$ = measurement sensitivity matrix
$\mathbf{I}$ = identity matrix
k = scalar filter gain
$\mathbf{K}$ = filter gain matrix
$\mathbf{P}$ = error covariance matrix
$\mathbf{P}_{ss}$ = steady-state error covariance matrix
$(\boldsymbol{q}, q_4)$ = quaternion parameterization of the true spacecraft attitude, C_{bI}
$(\hat{\boldsymbol{q}}, \hat{q}_4)$ = quaternion parameterization of the gyro spacecraft attitude estimate, $\hat{C}_{bI}^{G}$
q = process noise scalar
$\mathbf{Q}$ = process noise covariance matrix
r = measurement noise scalar
$\mathbf{R}$ = measurement noise covariance matrix
t_k = kth sample time
t^* = switching time
ΔT = sample period
$\boldsymbol{u}$ = gyro correction parameter
$\mathbf{W}(\boldsymbol{\alpha})$ = rotational kinematic matrix corresponding to the vector parameterization, $\boldsymbol{\alpha}$
$\boldsymbol{v}_p$ = external measurement noise
$\boldsymbol{w}_{\omega}$ = gyro measurement noise vector
$\boldsymbol{y}$ = attitude error measurement vector
$\boldsymbol{\alpha}$ = any vector parameterization of the true attitude C_{bI}
$\hat{\boldsymbol{\alpha}}$ = any vector parameterization of the gyro spacecraft attitude estimate, $\hat{C}_{bI}^{G}$
$(\boldsymbol{\varepsilon}, \eta)$ = quaternion parameterization of the gyro attitude estimate error, δC^{G}
$(\boldsymbol{\varepsilon}_{GM}, \eta_{GM})$ = quaternion parameterization of the measured gyro attitude estimate error, δC^{GM}
$(\boldsymbol{\varepsilon}_{M}, \eta_{M})$ = quaternion parameterization of the external attitude measurement error, δC^{M}

$\boldsymbol{\omega}$	=	spacecraft angular velocity vector expressed in body coordinates
$\boldsymbol{\omega}^m$	=	measured angular velocity vector
$\bar{\boldsymbol{\omega}}$	=	propagated angular velocity vector
$\boldsymbol{\Phi}$	=	state-transition matrix
σ	=	scalar covariance (positive)

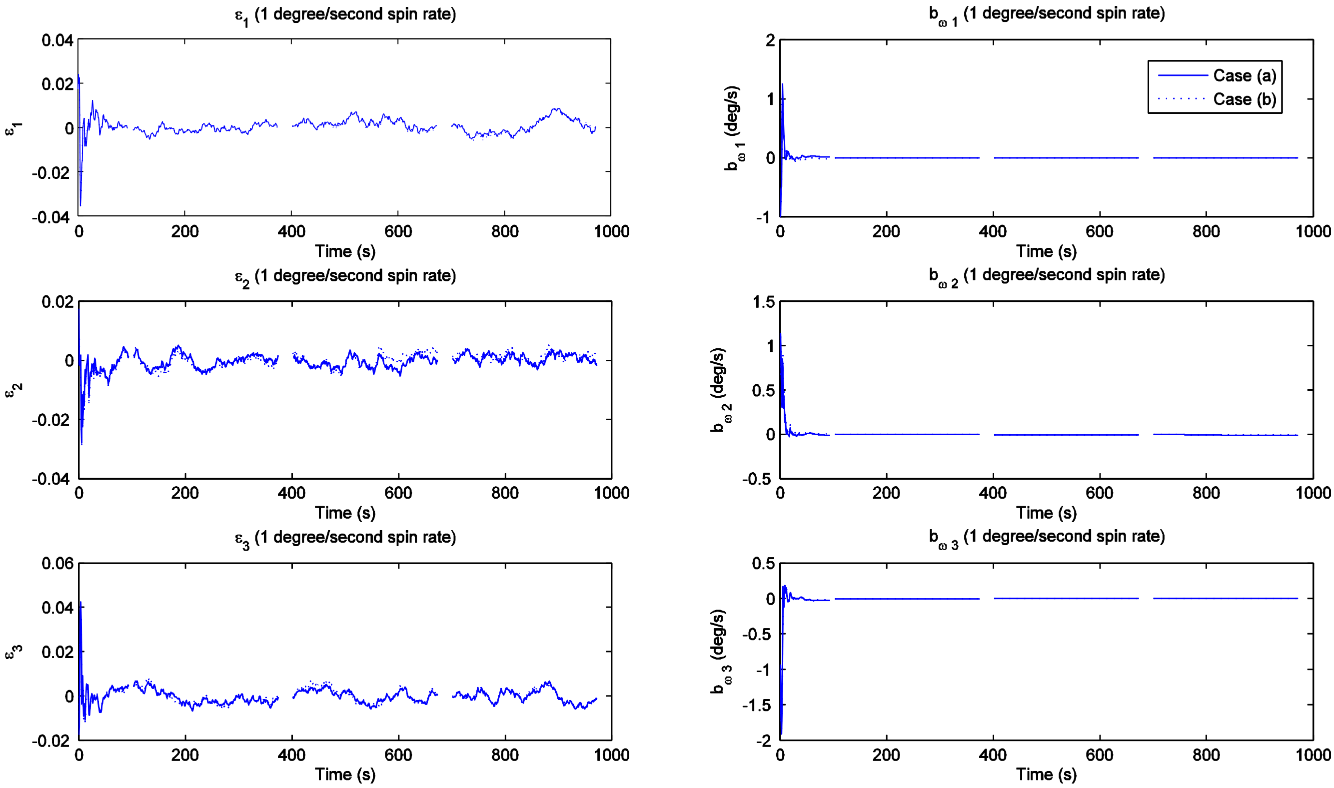

Figure 1: Estimation Errors for a 1 degree/second satellite spin rate about the body x-axis

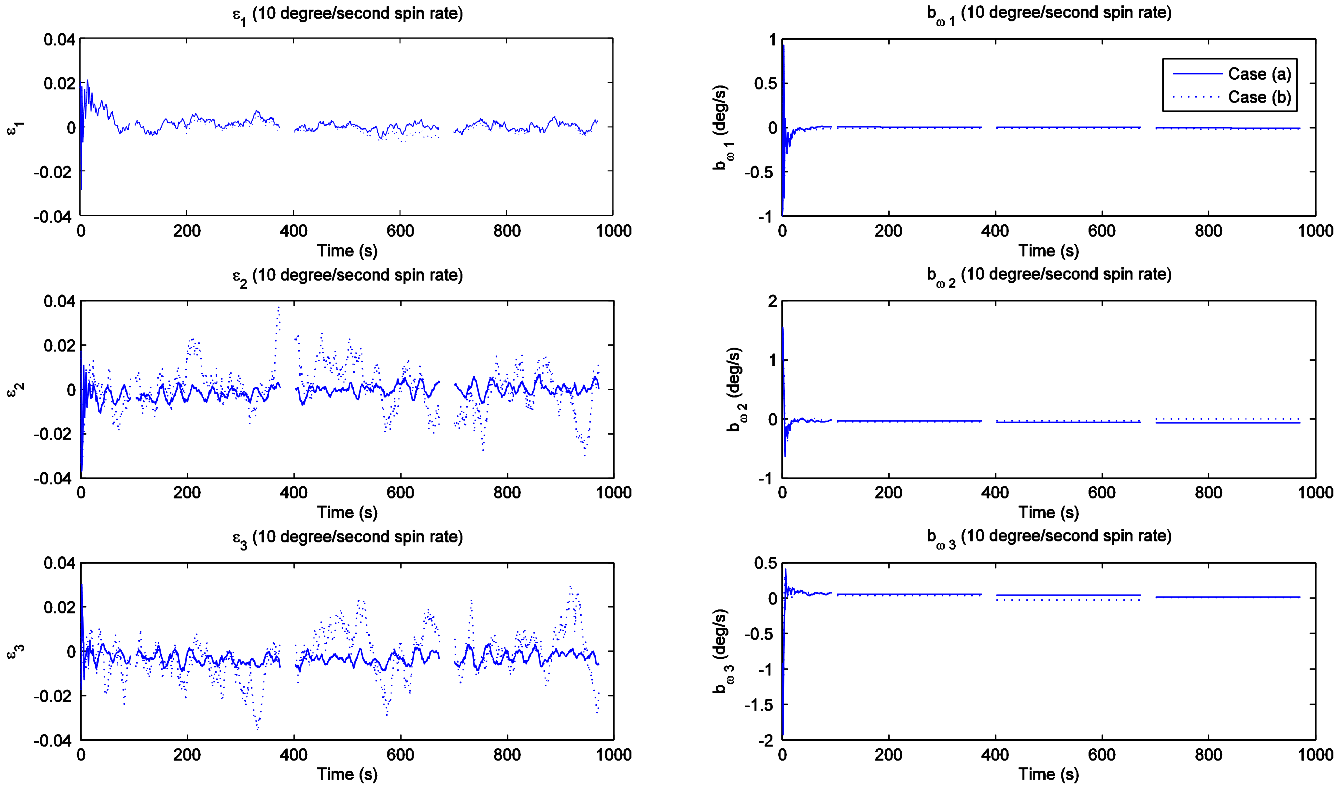

Figure 2: Estimation Errors for a 10 degree/second satellite spin rate about the body x-axis

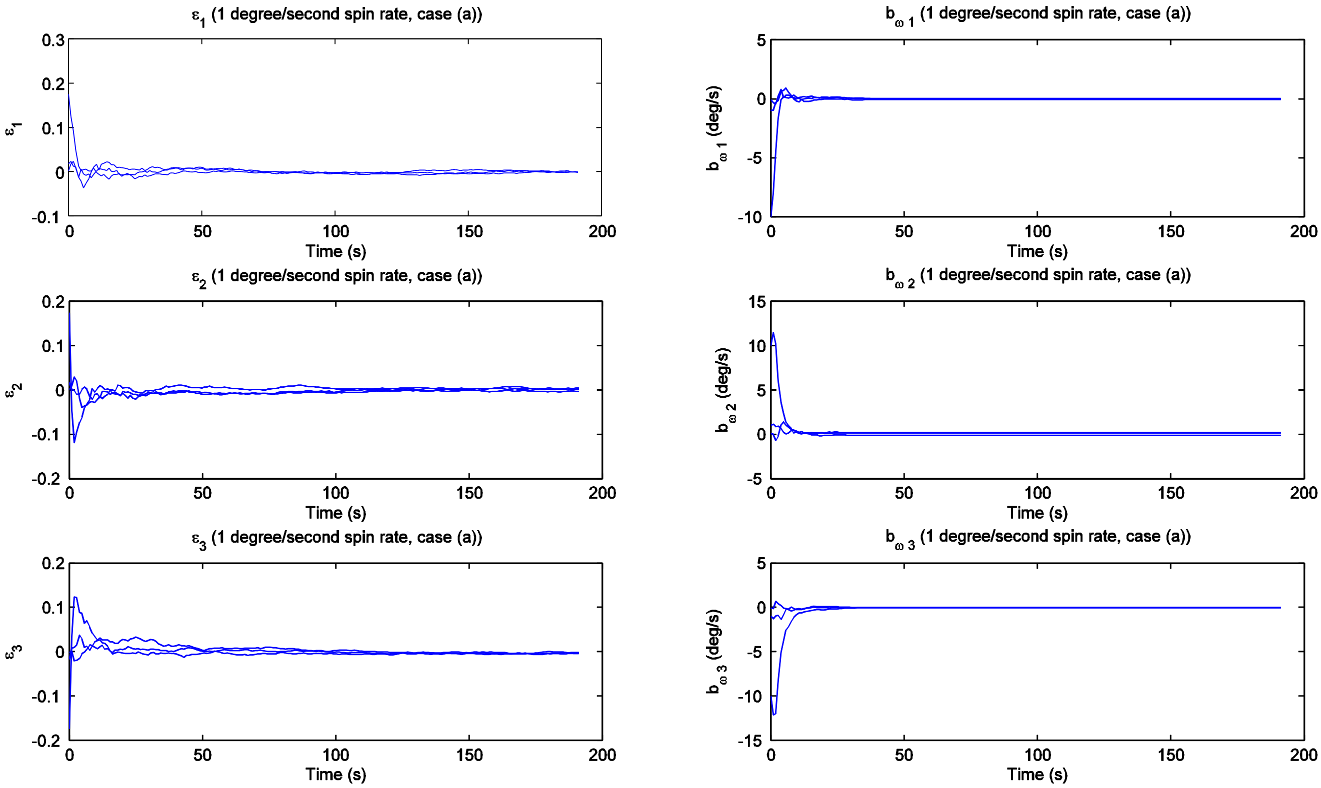

Figure 3: Estimation Errors case (a) with varying initial estimation uncertainties

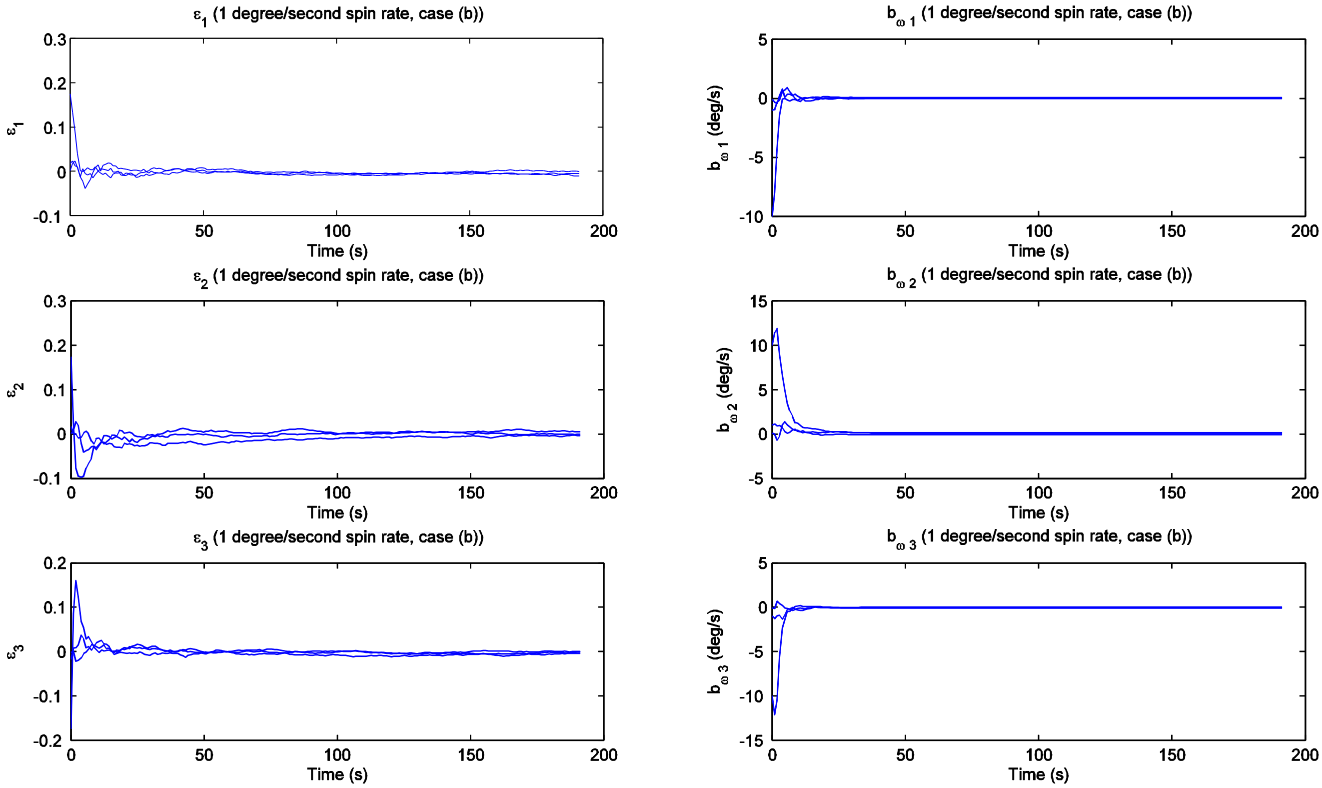

Figure 4: Estimation Errors case (b) with varying initial estimation uncertainties

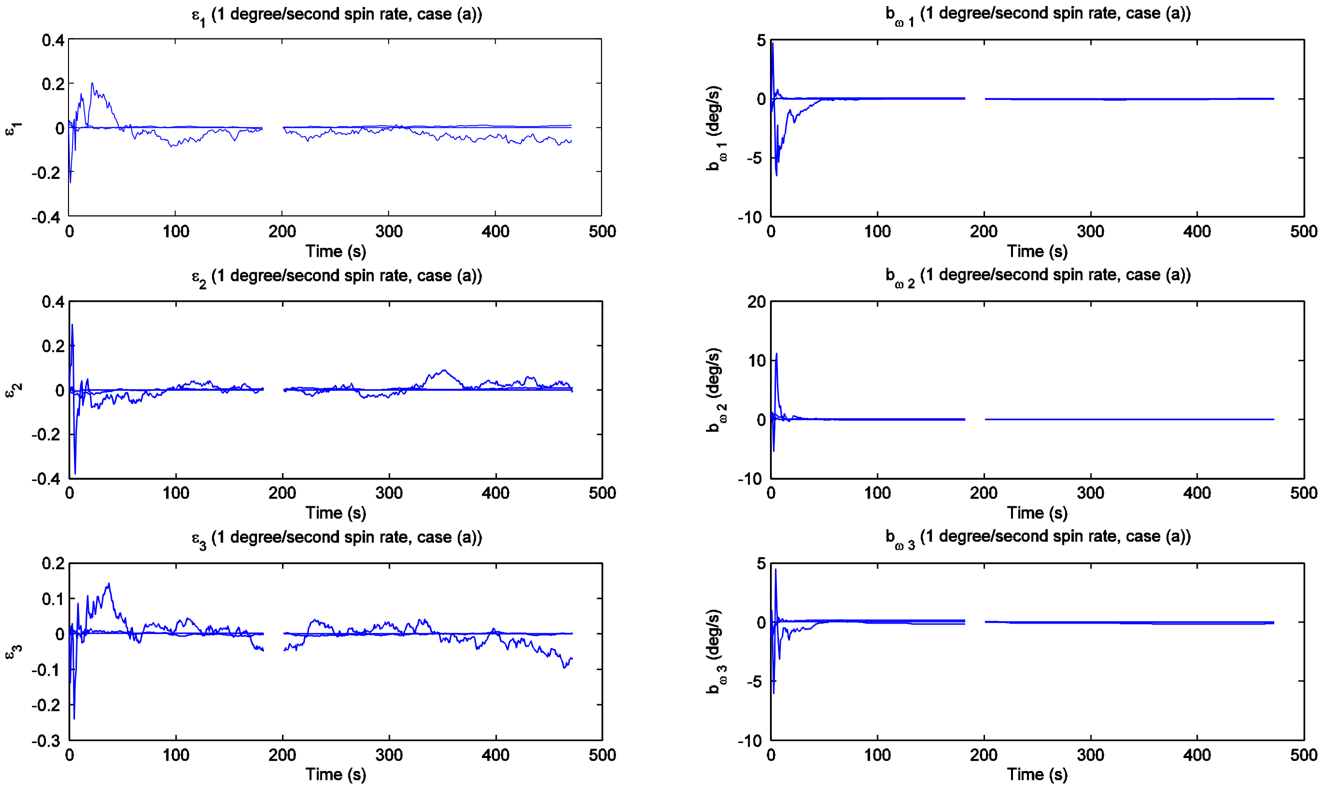

Figure 5: Estimation Errors case (a) with varying measurement noise covariances

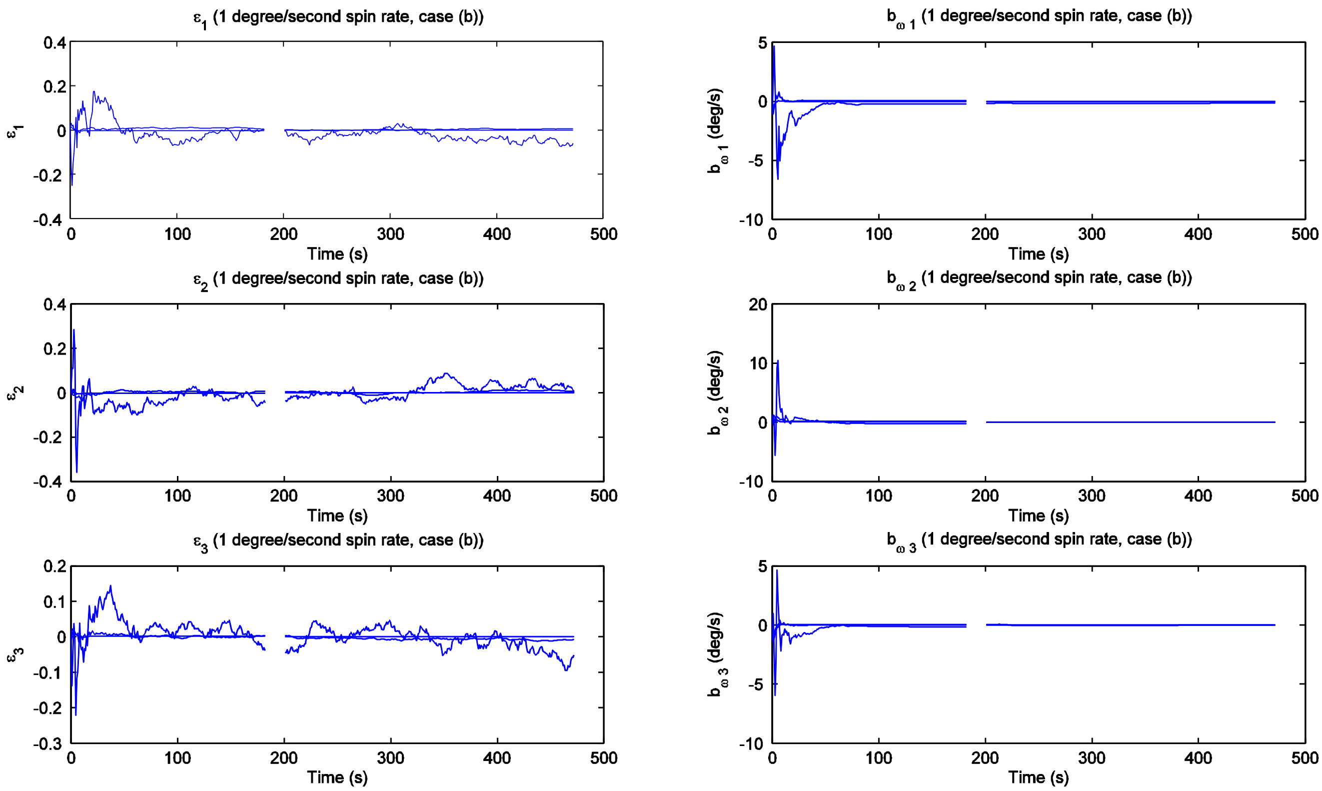

Figure 6: Estimation Errors case (b) with varying measurement noise covariances